Indian Journal of Pure & Applied Physics
Vol. 46, March 2008, pp. 176-186

Fractional order Fourier transform-based fringe-adjusted joint transform correlator

Alpana Bhagatji, Naveen K Nishchal[1], Arun K Gupta*& B P Tyagi[2]

Photonics Division, Instruments Research & Development Establishment, Raipur Road, Dehradun 248 008

[1]Department of Physics, Indian Institute of Technology Guwahati, Guwahati

[2]Department of Physics, D B S (PG) College, Dehradun

*E-mail: akgupta@irde.res.in

Received 22 August 2007; accepted 4 January 2008

An extended fractional Fourier transform (FRT) based fringe-adjusted joint transform correlator (JTC) for real-time target recognition applications has been implemented. In real-time situation, the input scene is captured using a charge-coupled device camera. The joint input images are fractional Fourier transformed and the joint power spectrum (JPS) has been recorded. Thus obtained JPS is multiplied by a pre-synthesized fringe-adjusted filter (FAF) to yield fractional fringe-adjusted JPS (FrFJPS). The FRT based fringe-adjusted JTC (FrFJTC) has been found to yield better results in comparison to the conventional fringe-adjusted JTC (FJTC). Three performance measure parameters; correlation peak intensity, peak-to-correlation energy and peak-to-sidelobe ratio have been calculated. Computer simulation and experimental results are presented.

Keywords: Joint transform correlator, Fringe-adjusted filter, Fractional Fourier transform

1 Introduction

One of the most important applications of optical information processing is optical pattern recognition[1-25]. The optical implementation of correlation can be accomplished either by using Fourier domain complex matched filtering or spatial domain filtering. Correlator that uses Fourier domain matched filtering is commonly known as VanderLugt correlator (VLC). An example of the spatial domain filtering is the joint transform correlator (JTC). The main advantage of JTC is that it does not require *a priori* filter fabrication and also relaxes the precise matching requirement of VLC. But one of the main problems associated with JTC is the presence of strong zero-order *dc* in the output plane, which overshadows the desired correlation peaks. There have been attempts to overcome this shortcoming[2-13]. Javidi and Kuo[2] proposed a binary JTC (BJTC), which is found to be superior to a classical JTC in terms of correlation peak intensity, correlation width and discrimination sensitivity. However in BJTC, binarization of the joint power spectrum (JPS) introduces harmonic correlation peaks that may cause false alarms[3,4]. To enhance the performance of classical and binary JTCs, Alam *et al.*[7-11] proposed fringe-adjusted joint transform correlator (FJTC) where the JPS is multiplied by a real-valued fringe-adjusted filter (FAF). A wavelet-modified FJTC has been proposed in our recent paper, which yields better results in comparison to conventional[13] FJTC.

The fractional Fourier transform (FRT) is a generalization of the conventional Fourier transform (FT). It was defined mathematically by Namias[14] and introduced to optics by Mendlovic *et al*[15-17]. The optical definition of FRT can be established through a phase-space rotation of the Wigner distribution function[18]. A generalized FRT, called extended[24] FRT, was also introduced to understand the optical transform between arbitrary planes on two sides of a lens. FRT has received considerable attention because of its application in imaging[19], analyzing beam propagation, lens designing and filtering. On the basis of the FRT operation, the classical correlation operation has been generalized to fractional correlation (FC). Since classical correlation is a shift-invariant operation, the location of the correlator output moves if the object translates at the input plane. For several pattern-recognition applications the shift-invariance property within the entire input plane is not necessary. Because of the shift-variance property of the FRT, FC makes shift-variant object recognition possible. The optical implementation of FRT in both VLC and JTC architectures has been reported[21-23].

In this paper, we demonstrate an extended FRT based FJTC for target recognition. The joint input

images are fractional Fourier transformed. The obtained fractional JPS (FrJPS) is multiplied by the FAF to yield fractional fringe-adjusted JPS (FrFJPS). For computer simulation, the obtained FrFJPS is inverse Fourier transformed and for experimental implementation, the FrFJPS is inverse fractional Fourier transformed. The two correlation peaks and *dc* are obtained in the correlation plane. The FRT based FJTC has been found to yield better results in comparison to conventional FJTC. Three performance measure parameters; correlation peak intensity, peak-to-correlation energy and peak-to-side lobe ratio have been calculated for conventional FJTC and FrFJTC.

2 Extended FRT

The a^{th} order FRT of a function $f(x)$ is given[21] by :

$$F^{a}\left[f(x)\right] = g(u) = \int_{-\infty}^{+\infty} f(x)\exp\left[i\pi\left(\frac{x^2+x'^2}{T}\right) - i2\pi\frac{xx'}{S}\right]dx' \quad \ldots(1)$$

with $T = \lambda f_1 \tan(\phi)$ and $S = \lambda f_1 \sin(\phi)$ where λ is the wavelength of light and $f_1 = f/\tan(\phi/2)$, f being the focal length of the lens. The fraction a is associated with a rotation in the Wigner distribution by an angle $\phi = a\pi/2$. Some of the essential properties of FRT are: (i) it is linear, (ii) the first order transform (a=1) corresponds to the classical FT, and (iii) it is additive in index, $F^{a1}F^{a2}[f(x)] = F^{a1+a2}[f(x)]$.

The extended FRT of a function $f(x)$ is given[24] by :

$$g(u) = K\int_{-\infty}^{+\infty} f(x)\exp(i\pi\frac{a^2x^2+b^2u^2}{\tan\alpha} - i2\pi\frac{abxu}{\sin\alpha})dx \quad \ldots(2)$$

where a, α, and b are the three parameters (called quadratic phase system, QPS parameters) of the FRT; K is a complex constant; and a, α, and b are in general complex quantities. We follow a one-dimensional representation for convenience and clarity. Performing an extended FRT on a function is equivalent to expanding the function a times, performing an FRT of order α, and contracting the resultant distribution b times. The parameters a, α, and b are related to the distances d_1 and d_2 and the focal length[24] f of the lens L (shown in Fig. 1) through Eqs (2-4) :

$$a^2 = \frac{1}{\lambda}\frac{\sqrt{f-d_2}}{\sqrt{f-d_1}}\frac{1}{\left[f^2-(f-d_1)(f-d_2)\right]^{1/2}} \quad \ldots(3)$$

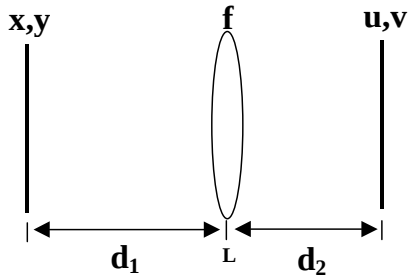

Fig. 1 — Optical set-up for extended FRT

$$\alpha = \arccos\left(\frac{\sqrt{f-d_1}\sqrt{f-d_2}}{f}\right) \quad \ldots(4)$$

$$b^2 = \frac{1}{\lambda}\frac{\sqrt{f-d_1}}{\sqrt{f-d_2}}\frac{1}{\left[f^2-(f-d_1)(f-d_2)\right]^{1/2}} \quad \ldots(5)$$

where λ expresses the wavelength.

3 Fractional Fourier Transform based Fringe-adjusted JTC

Let $r(x-l, y+m)$ denote the reference-image function and $t(x+l, y-m)$ represent the target-image function. The input joint-image function $f(x,y)$ can be expressed as:

$$f(x,y) = r(x-l,y+m)+t(x+l,y-m) \quad \ldots(6)$$

The FRT of the input joint-image function is given as:

$$F(u,v) = \mathrm{FRT}^{(a,\alpha,b)}[f(x,y)] \quad \ldots(7)$$

where (u,v) are the frequency-domain co-ordinates and $[a,\alpha,b]$ are the QPS parameters of FRT. The fractional JPS captured by an intensity sensing device, CCD camera, at the fractional Fourier plane is given as:

$$I(u,v) = |F(u,v)|^2 \quad \ldots(8)$$

For FrFJTC, the fractional JPS so obtained is multiplied by real-valued[7] FAF given as :

$$H_{faf}(u,v) = \frac{B(u,v)}{A(u,v)+|R(u,v)|^2} \quad \ldots(9)$$

where $A(u,v)$ and $B(u,v)$ are constants, and $|R(u,v)|$ is the amplitude of reference image at fractional Fourier plane. A small value of $A(u,v)$ overcomes the pole

problem and it is also possible to achieve high autocorrelation peaks. The value of $B(u,v)$ is properly selected to avoid optical gain greater than unity. If $B(u,v) = 1$ and $|R(u,v)|^2 >> A(u,v)$, the $H_{faf}(u,v)$ given in Eq. (9) may be written as:

$$H_{\text{faf}}(u,v) = \frac{1}{\left|R(u,v)\right|^2} \qquad \ldots(10)$$

The fractional JPS multiplied by FAF results into fractional fringe-adjusted JPS (FrFJPS) given as:

$$\text{FrFJPS} = I(u,v) \times H_{\text{faf}}(u,v) \qquad \ldots(11)$$

On inverse transformation, FrFJPS, given in Eq. (11), results into *dc* and two correlation peaks.

4 Experimental Details

The performance of FrFJTC for target recognition has been investigated and the results obtained were compared with FJTC. A FAF was synthesized taking the value of $A(u, v)$ equal to 1×10^{-1} to overcome the pole problem and $B(u, v)$ was set to unity.

The noise-free gray level images of five tanks viz. tank 1, tank 2, tank 3, tank 4 and tank 5 [Figs 2(a-e)], each of size 100 × 45 pixels, were used to perform the study. The following cases were considered for joint input images (i) tank 1 with same tank and tank 1 with different tank (tank 2), (ii) tank 2 with same tank and tank 2 with different tank (tank 3), (iii) tank 3 with same tank and tank 3 with different tank (tank 4), (iv) tank 4 with same tank and tank 4 with different tank (tank 5), (v) tank 5 with same tank and tank 5 with different tank (tank 1). In case (i), tank 1 was used as reference image and in cases (ii) to (v), tank 2 to tank 5, respectively were taken as reference images. The reference and input images were combined and zero-padded to form a joint image of size 256 × 256 pixels.

The experimental set-up used for implementing FJTC and FrFJTC is shown in Fig. 3. A beam from a laser-diode source (λ = 670 nm) is expanded and then collimated using a collimating lens of focal length 75 mm. This collimated laser beam illuminates a reflection-type, gray-level, ferro-electric liquid-crystal BNS (Boulder Nonlinear System, USA) SLM of size 256 × 256 pixels (with pixel size 18 × 18 μm) used to display input joint-image. A Fourier transforming lens of focal length 135 mm takes the Fourier transform in case of FJTC. For FrFJTC, the same lens is used to take the FRT but placed at a distance d_1 equal to

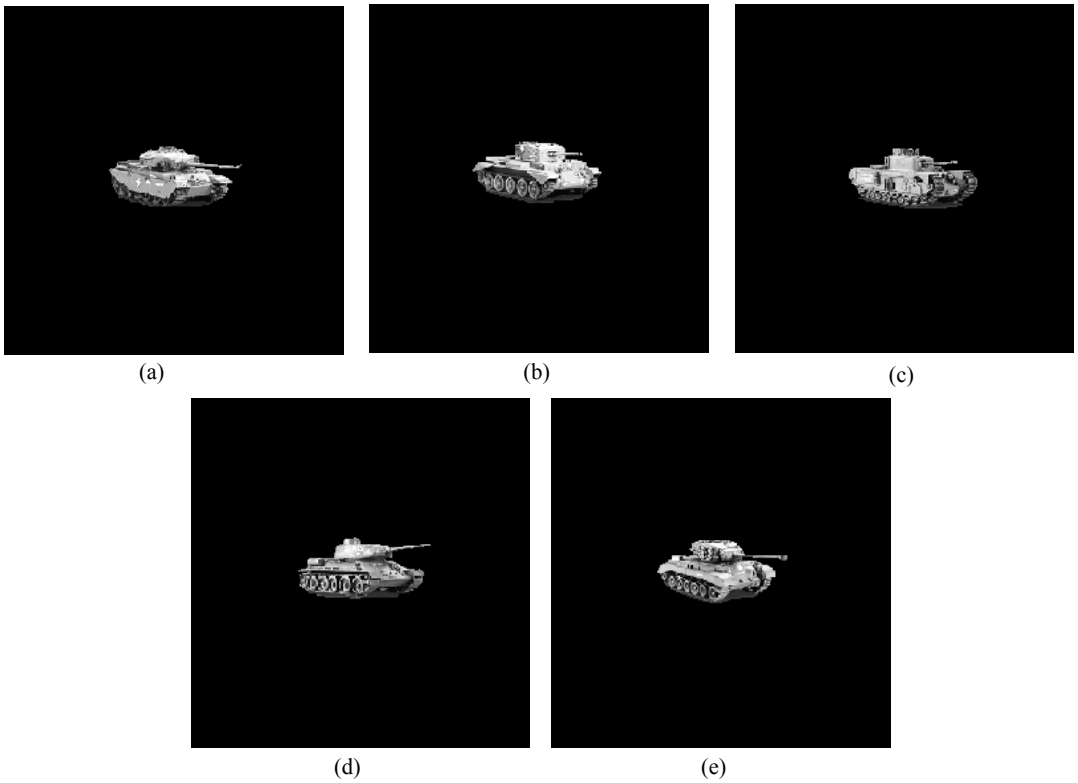

Fig. 2 — Images of tanks (a) tank 1, (b) tank 2, (c) tank 3, (d) tank 4, and (e) tank 5

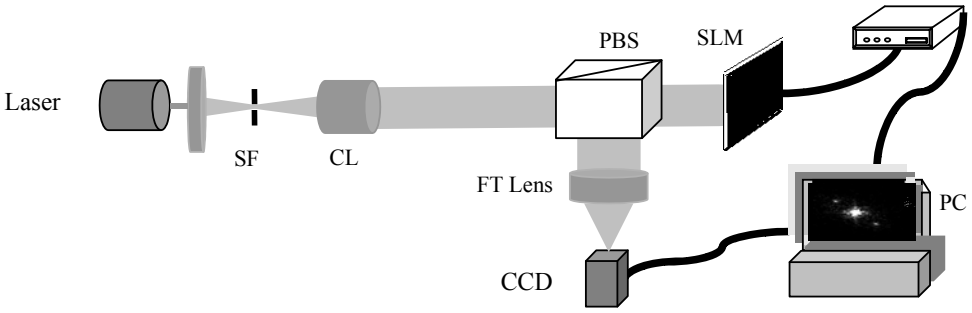

Fig. 3 — Experimental set-up. SF: spatial filter; CL: collimating lens; PBS: polarizing beam splitter; FT lens: Fourier transform lens

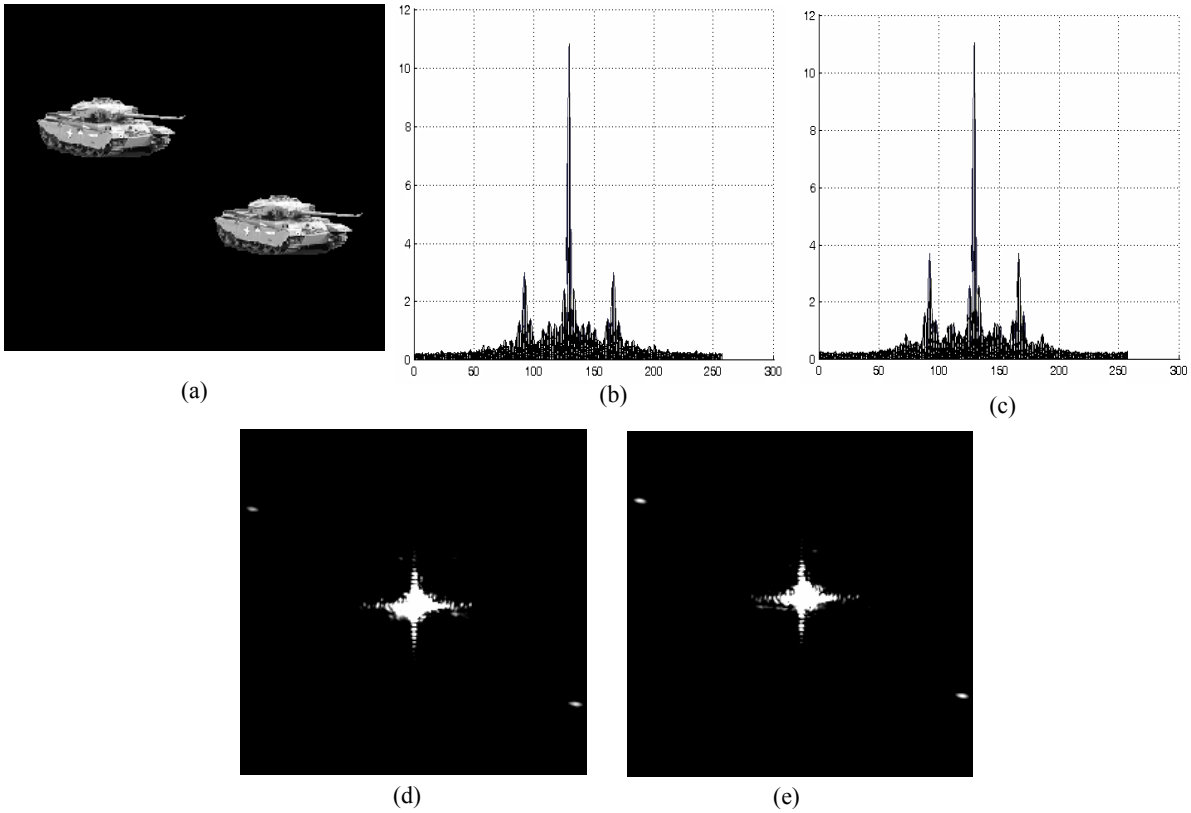

Fig. 4 — (a) Input images having reference (tank 1) and target (tank 1); corresponding simulation results (b) FJTC, (c) FrFJTC, and corresponding experimental results (d) FJTC, (e) FrFJTC.

192 mm from the SLM. The JPS (and correlation peaks) are captured using a CCD camera of size 752 × 582 pixels (Sony, Japan: pixel size 6.5 × 6.25 μm) connected to a PC through a frame-grabber card. For FrFJTC, the FrFJPS (and correlation peaks) are captured at a distance d_2 equal to 139 mm from the FT lens. The parameters of QPS as calculated from Eqs (3-5) using f =135 mm, d_1 192 mm, d_2 =139 mm, and λ = 670 nm are a = 1.7168, α = 1.6829, and b = 6.4806.

Figure 4 (a) shows the input joint-image of tank 1 with the same tank. This input image was displayed onto the SLM to obtain JPS and FrJPS. The captured JPS and FrJPS were multiplied digitally by FAF before taking the inverse Fourier transformation. Figure 4(b,c) show the simulation results obtained on taking the inverse Fourier transform of FJPS and FrFJPS, respectively. The correlation peak of magnitude 3.0120 and 3.7026 arbitrary units (au) was obtained for FJTC and FrFJTC, respectively. The simulation was performed on MATLAB platform. From the results, it is observed that the correlation peak height is enhanced for FrFJTC in comparison to FJTC. Fig. 4(d) shows the experimental result obtained on optical inverse Fourier transformation of FJPS. The experimental result achieved on inverse

FRT of FrFJPS is shown in Fig. 4(e). The intensity of the correlation peaks for FrFJTC is enhanced in comparison to FJTC. Figure 5(a) shows the input joint-image of tank 1 with a different tank (tank 2). The corresponding simulation and experimental results for FJTC and FrFJTC are shown in [Figs 5(b, c) and 5(d, e)], respectively.

Another case in which tank 2 was taken as the reference image was considered. The input joint image comprising of tank 2 versus tank 2 (Fig. 6(a)) and tank 2 versus tank 3 [Fig. 7(a)] were fed onto the SLM. The JPS and FrJPS were captured and multiplied digitally by FAF to obtain FJPS and FrFJPS, respectively. The obtained power spectra were inverse Fourier transformed and the corresponding simulation results are shown in [Figs 6(b,c) and Figs 7(b,c)]. The correlation peak value of 3.868 and 4.4035 au was obtained for FJTC and FrFJTC for the joint input of Fig. 6(a). Thus, FrFJTC yields the best result. The corresponding experimental results obtained on optical inverse Fourier transformation of FJPS are shown in [Figs 6(d) and 7(d)], respectively. Figs 6(e) and Figs 7(e) show the experimental results achieved on optical inverse FRT of FrFJPS.

Similar study was carried out for other three cases (iii-v). The joint input image, corresponding simulation and experimental results for the case tank 3 versus tank 3 and tank 3 versus tank 4 are shown in [Figs 8(a-e) and 9(a-e)], respectively. [Figs 10(a-e) and 11(a-e)] show the joint images and the corresponding results for tank 4 with the same tank and tank 4 with different tank (tank 5). The results yielded for tank 5 versus tank 5 (Fig. 12 (a)) and tank 5 versus tank 1 [Fig. 13(a)] are shown in [Figs 12 (b-e) and 13(b-e)] respectively.

The results obtained with FrFJTC are comparable to our previous work on wavelet-modified[13] FJTC. The correlation peak value equal to 3.715 au for the joint input of tank 1 versus tank 1 using wavelet-modified FJTC is quite comparable to the value equal to 3.702 au obtained for the same joint input using FRT based FJTC. To note that in case of FRT based FJTC no extra software or hardware is required for the implementation of FRT. Therefore, the computation time required for processing the FJPS

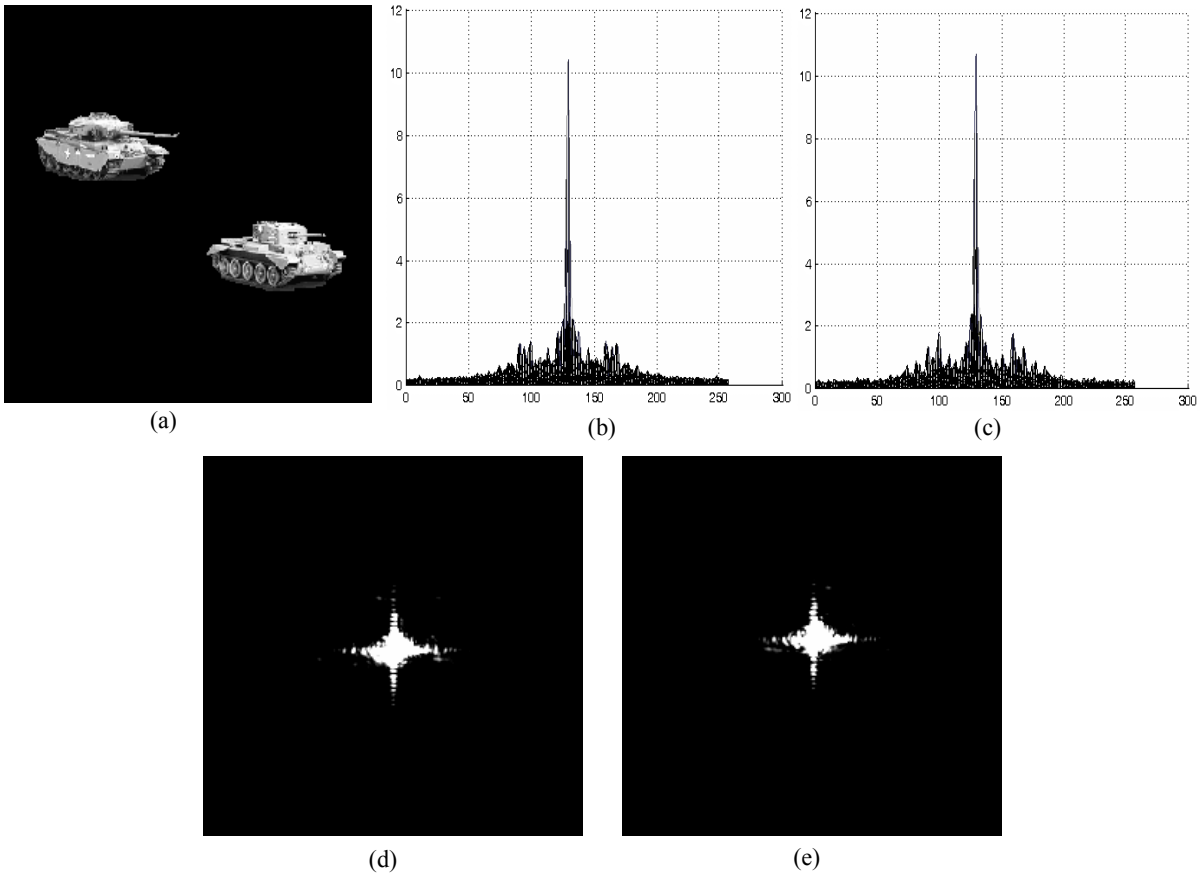

Fig. 5 — (a) Input images having reference (tank 1) and target (tank 2); corresponding simulation results (b) FJTC, (c) FrFJTC, and corresponding experimental results (d) FJTC, (e) FrFJTC

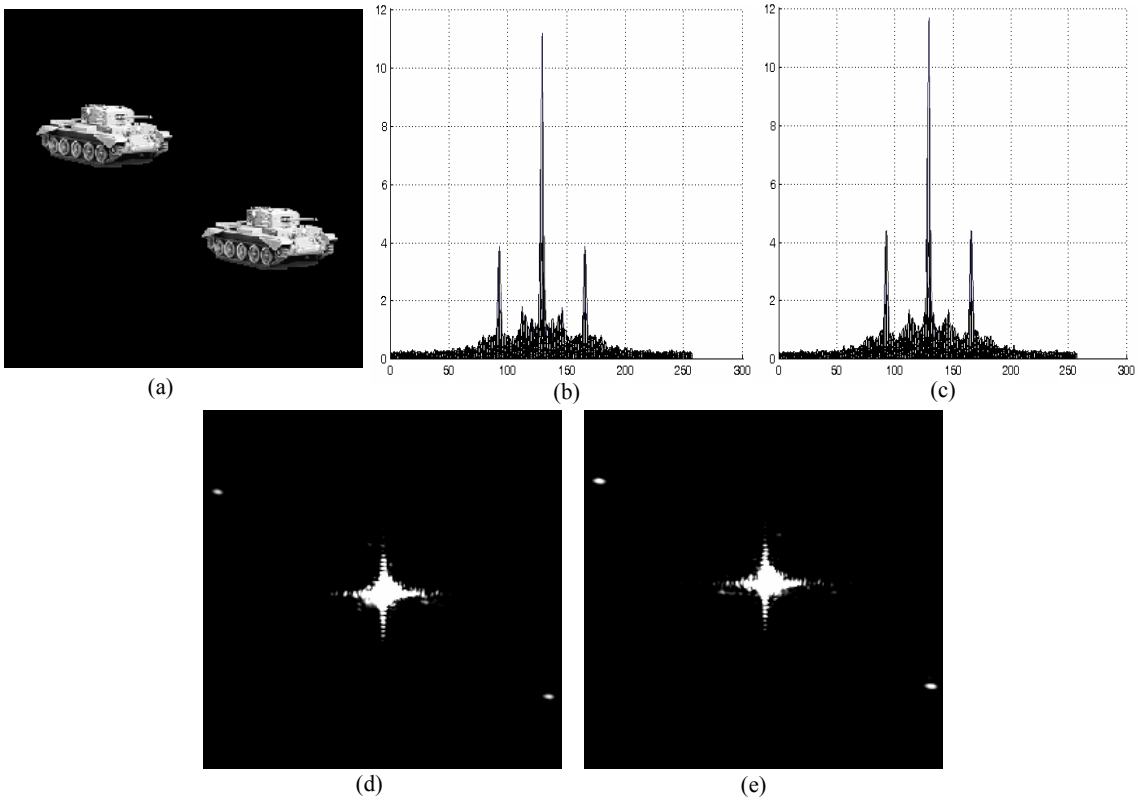

Fig. 6 — (a) Input images having reference (tank 2) and target (tank 2); corresponding simulation results (b) FJTC, (c) FrFJTC, and corresponding experimental results (d) FJTC, (e) FrFJTC

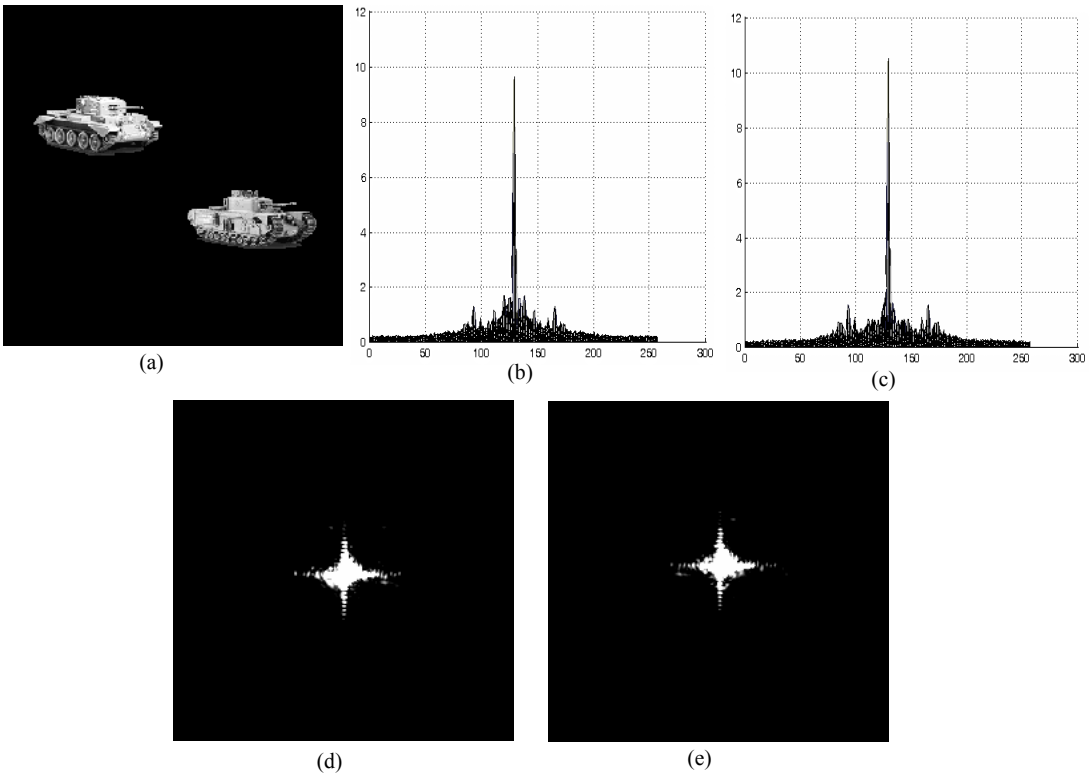

Fig. 7 — (a) Input images having reference (tank 2) and target (tank 3); corresponding simulation results (b) FJTC, (c) FrFJTC, and corresponding experimental results (d) FJTC, (e) FrFJTC

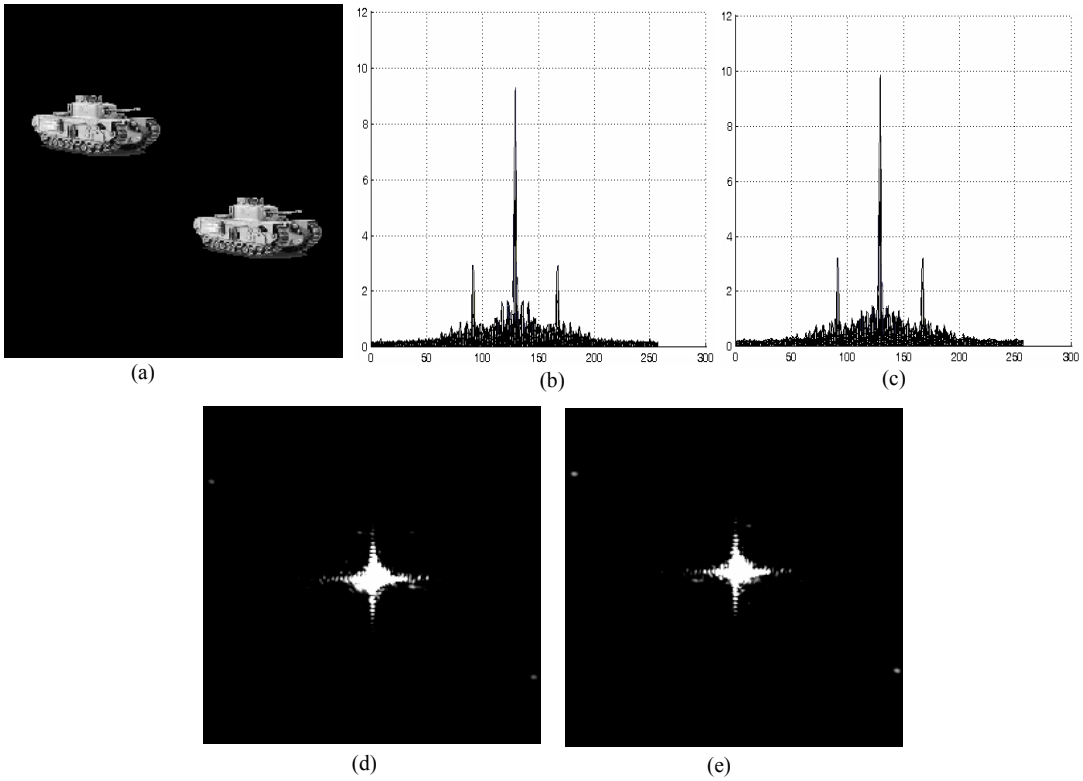

Fig. 8 — (a) Input images having reference (tank 3) and target (tank 3); corresponding simulation results (b) FJTC, (c) FrFJTC, and corresponding experimental results (d) FJTC, (e) FrFJTC.

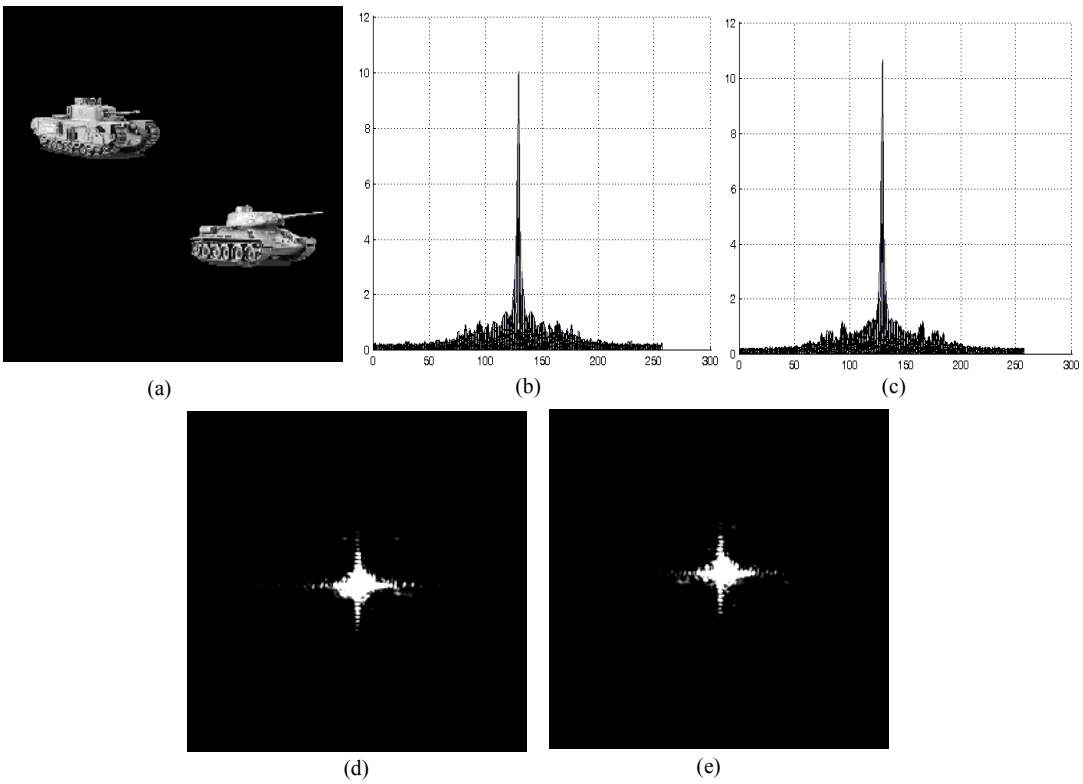

Fig. 9 — (a) Input images having reference (tank 3) and target (tank 4); corresponding simulation results (b) FJTC, (c) FrFJTC, and corresponding experimental results (d) FJTC, (e) FrFJTC

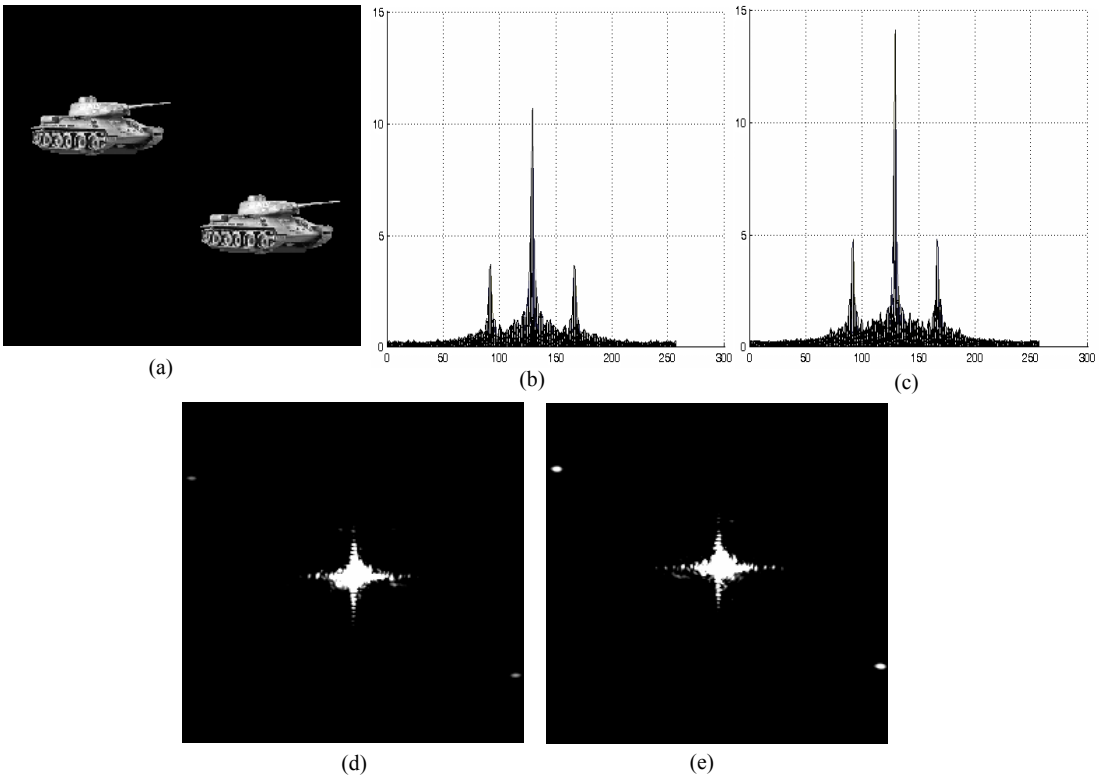

Fig. 10 — (a) Input images having reference (tank 4) and target (tank 4); corresponding simulation results (b) FJTC, (c) FrFJTC, and corresponding experimental results (d) FJTC, (e) FrFJTC

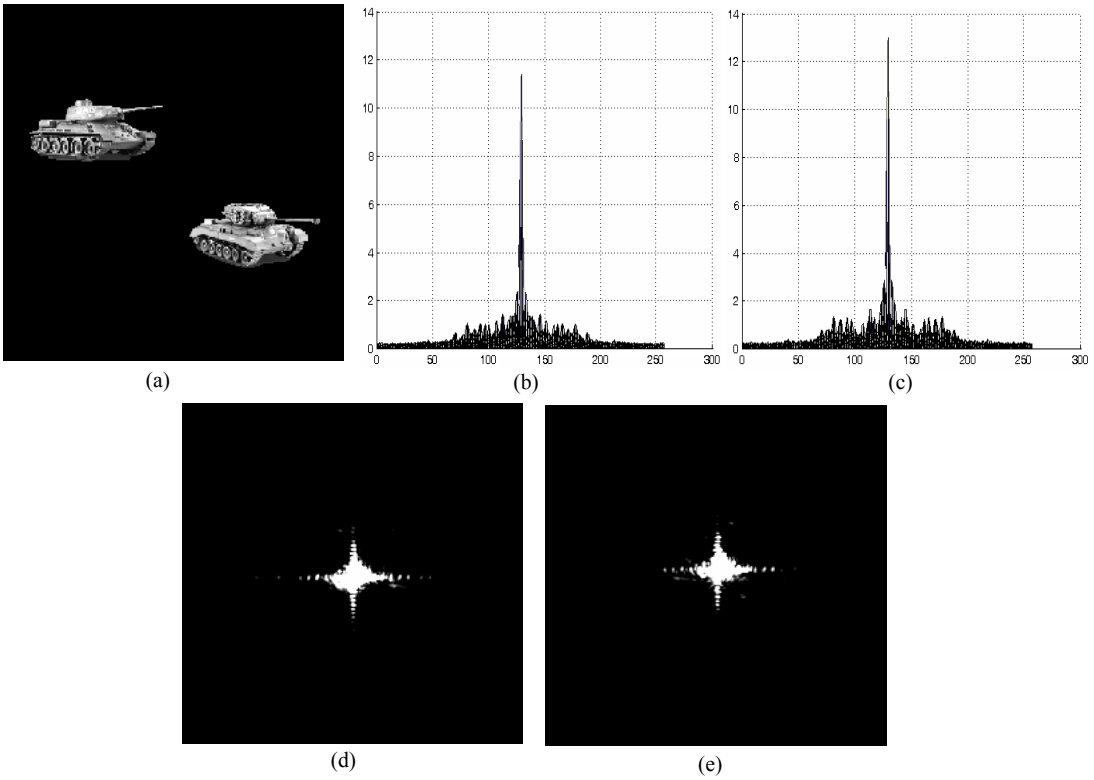

Fig. 11 — (a) Input images having reference (tank 4) and target (tank 5); corresponding simulation results (b) FJTC, (c) FrFJTC and corresponding experimental results, (d) FJTC, (e) FrFJTC

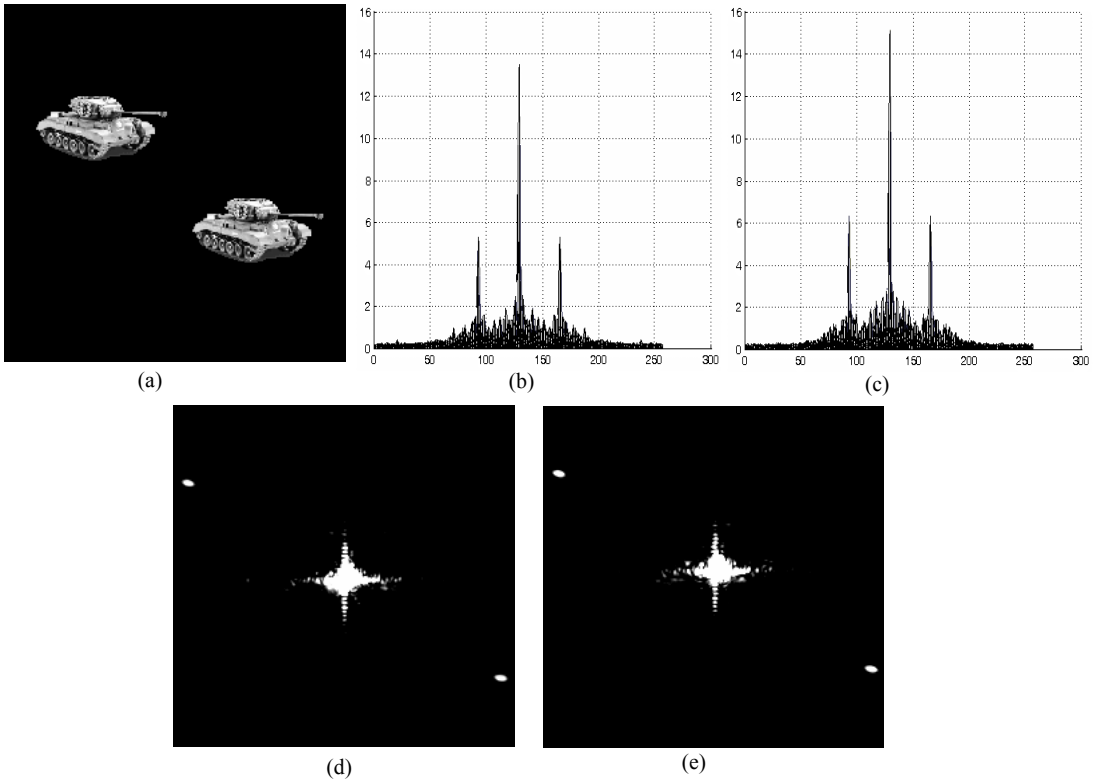

Fig. 12 — (a) Input images having reference (tank 5) and target (tank 5); corresponding simulation results (b) FJTC, (c) FrFJTC, and corresponding experimental results (d) FJTC, (e) FrFJTC

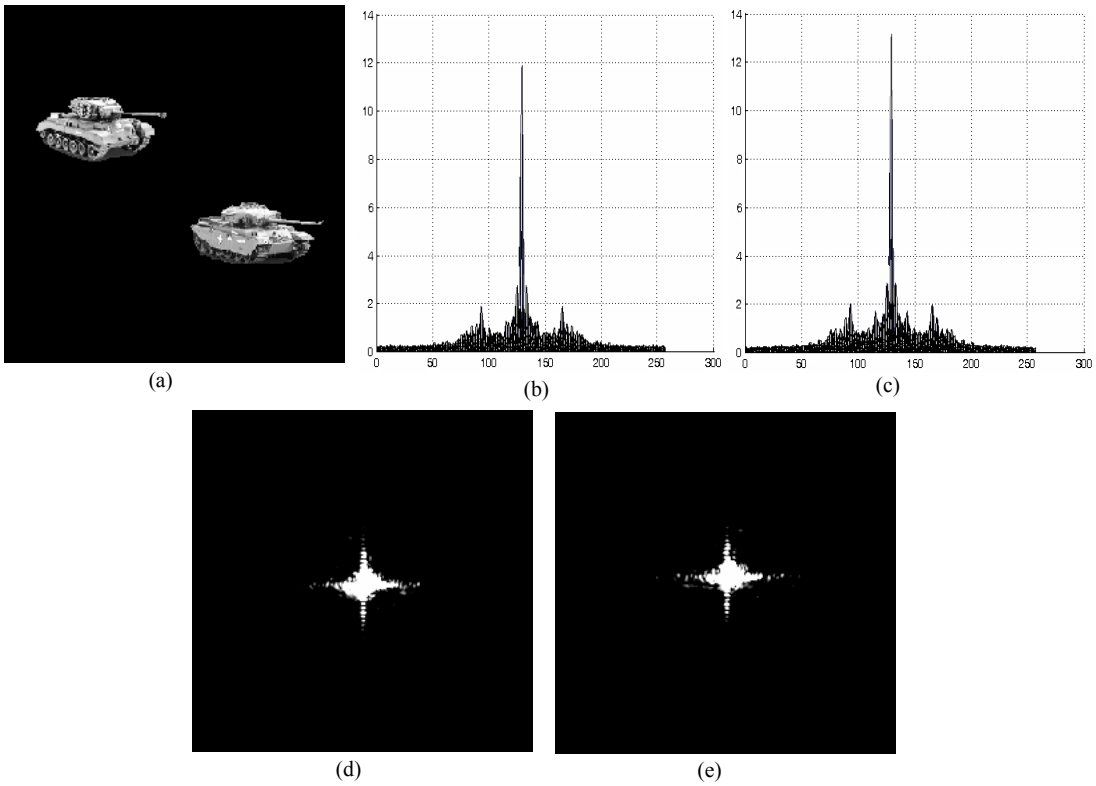

Fig. 13 — (a) Input images having reference (tank 5) and target (tank 1); corresponding simulation results (b) FJTC, (c) FrFJTC, and corresponding experimental results (d) FJTC, (e) FrFJTC.

Table 1 — Calculated values of CPI for different joint input images

Joint input image	CPI	
	FJTC	FrFJTC
Tank 1 vs Tank 1	9.072	13.709
Tank 2 vs Tank 2	14.961	19.391
Tank 3 vs Tank 3	8.679	10.371
Tank 4 vs Tank 4	13.546	22.978
Tank 5 vs Tank 5	28.386	40.139

Table 2 — Calculated values of PCE for different joint input images

Joint input image	PCE	
	FJTC	FrFJTC
Tank 1 vs Tank 1	0.0044	0.0066
Tank 2 vs Tank 2	0.0070	0.0087
Tank 3 vs Tank 3	0.0051	0.0058
Tank 4 vs Tank 4	0.0067	0.0083
Tank 5 vs Tank 5	0.0106	0.0135

with an appropriately scaled wavelet filter can be averted in case of FRT based FJTC.

5 Performance Study

Three parameters-correlation peak intensity (CPI), peak-to-correlation energy (PCE), and peak-to-sidelobe ratio (PSR) have been calculated to check the performance of FJTC and FrFJTC. The CPI is defined as the square of the magnitude of correlation peak. The PCE is defined as the ratio of correlation peak intensity value to the total energy of correlation plane. The PSR is defined as the ratio of the magnitude of the correlation peak, minus the mean of the sidelobe window, to the standard deviation of the sidelobe window. A sidelobe window of size 19 × 19 pixels was selected across the central peak (excluding the peak value). The computer simulation results were used for calculating these performance measures. All the calculated values for CPI, PCE, and PSR have been tabulated.

Table 1 gives the values of CPI for FJTC and FrFJTC when joint input images corresponding to [Figs 4(a), 6(a), 8(a), 10(a), and 12(a)] were considered. From the obtained values, we find that CPI is higher for FrFJTC as compared to FJTC. The PCE and PSR values have been presented in Tables 2 and 3, respectively. It is inferred that FrFJTC enhances the PCE and SCR values in comparison to FJTC (Tables 2 and 3).

Table 3 — Calculated values of PSR for different joint input images

Joint input image	PSR	
	FJTC	FrFJTC
Tank 1 vs Tank 1	10.938	13.051
Tank 2 vs Tank 2	18.119	19.976
Tank 3 vs Tank 3	13.570	16.029
Tank 4 vs Tank 4	14.624	16.369
Tank 5 vs Tank 5	17.291	19.603

6 Conclusion

In this paper, we have presented an extended FRT based FJTC for target recognition. It is found to yield better correlation output than FJTC. Three performance measure parameters; correlation peak intensity, peak-to-correlation energy and peak-to-side lobe ratio have been calculated for conventional FJTC and FrFJTC. The results obtained with FrFJTC are comparable to our previous work on wavelet-modified FJTC. To note that in case of FRT based FJTC, no extra software or hardware is required for the implementation of FRT. Therefore, the computation time required for processing the FJPS with an appropriately scaled wavelet filter can be averted in case of FRT based FJTC. The same architecture could be used for multiple target recognition applications.

Acknowledgement

The authors are grateful to Mr S S Sundaram, Director, Instruments Research and Development Establishment, Dehradun, for giving permission to publish this paper.

References

1 Yu F T S & Jutamulia S, Eds, *Optical Pattern Recognition* (Cambridge Univ Press, Cambridge, 1998).
2 Javidi B & Kuo C, *Appl Opt*, 27 (1988) 663.
3 Yu F T S, Cheng F, Nagata T & Gregory DA, *Appl Opt*, 28 (1989) 2988.
4 Hahn W B & Flannery D L, *Opt Eng*, 31 (1992) 896.
5 Pati G S & Singh K, *Opt Commun*, 147 (1998) 26.
6 Nishchal N K, Goyal S, Aran A, Beri V K & Gupta A K, *Opt Eng*, 45 (2006) 026401.
7 Alam M S & Karim M A, *Appl Opt*, 32 (1993) 4344.
8 Alam M S & Karim M A, *Opt Eng*, 33 (1994) 1610.
9 Chen X-W & Alam M S, *Opt Eng*, 37 (1998) 138.
10 Alam M S & Horache E H, *Opt Commun*, 236 (2004) 59.
11 Haider M R, Islam M N & Alam M S, *Opt Eng*, 45 (2006) 048201.
12 Wang Q, Deng Y & Liu S, *Opt Eng*, 45 (2006) 087002.
13 Bhagatji A, Nishchal N K, Gupta A K & Tyagi B P, *Opt Laser Technol*, 40 (2008) 99.

14 Namias V, *J Inst Math Appl*, 25 (1980) 241.
15 Ozaktas H M & Mendlovic D, *Opt Commun*, 110 (1993) 163.
16 Mendlovic D & Ozaktas H M, *J Opt Soc Am A*, 10 (1993) 1875.
17 Ozaktas H M & Mendlovic D, *J Opt Soc Am A*, 10 (1993) 2522.
18 Lohmann A W, *J Opt Soc Am A*, 10 (1993) 2181.
19 Bernardo L M & Soares O D, *J Opt Soc Am A*, 11 (1994) 2622.
20 Ozaktas H M, Zalevsky Z & Kutay M A, *The Fractional Fourier Transform with Applications in Optics and Signal Processing* (John Wiley, New York, 2001).
21 Mendlovic D, Bitran Y, Dorsch R G & Lohmann A W, *J Opt Soc Am A*, 12 (1995) 1665.
22 Lohmann A W & Mendlovic D, *Appl Opt*, 36 (1997) 7402.
23 Kuo C J & Luo Y, *Appl Opt*, 37 (1998) 8270.
24 Hua J, Liu L & Li G, *J Opt Soc Am A*, 14 (1997) 3316.
25 Jin W, Yan C, Ma L, Ye H & Wang H, *Opt Commun*, 268 (2006) 34.